Mem. S.A.It. Suppl. Vol. 1, 210

Memorie della
Supplementi

A new three-dimensional general-relativistic hydrodynamics code

L. Baiotti[1,2], I. Hawke[3], P.J. Montero[1], L. Rezzolla[1,2]

[1] SISSA, Via Beirut 2-4, 34014 Trieste, Italy

[2] INFN, Sezione di Trieste, Via Beirut 2-4, 34014 Trieste, Italy

[3] Albert-Einstein-Institut, Am Mühlenberg 1, 14476 Golm, Germany

Abstract. We present a new three-dimensional general relativistic hydrodynamics code, the `Whisky` code. This code incorporates the expertise developed over the past years in the numerical solution of Einstein equations and of the hydrodynamics equations in a curved spacetime, and is the result of a collaboration of several European Institutes. We here discuss the ability of the code to carry out long-term accurate evolutions of the linear and nonlinear dynamics of isolated relativistic stars.

Key words. relativistic hydrodynamics – numerical methods

1. Introduction

During the last few years, computational general relativistic astrophysics has become increasingly important and accurate. This is partly due to the rapid increase in computing power through massively parallel supercomputers which make large-scale, multi-dimensional numerical simulations possible (Font et al. 2000b; Shibata & Uryu 2000; Font et al. 2002; Shibata & Uryu 2002; Duez et al 2002). In addition to being a unique tool for investigating General Relativity in regimes of strong and rapidly varying gravitational fields, such simulations are also needed to fully understand the incoming wealth of observations from high-energy astronomy and (near-future) gravitational wave astronomy. In an attempt to respond, at least in part, to this need we have recently developed `Whisky`, a three-dimensional (3D) general relativistic hydrodynamics code. The `Whisky` code is the result of an ongoing collaboration among several European Institutes, i.e. the Albert Einstein Institute (Golm, Germany), SISSA (Trieste, Italy) and the Universities of Thessaloniki (Greece) and Valencia (Spain), joined in a European Network investigating sources of gravitational waves (see `www.eu-network.org` for further information).

In practice, the `Whisky` code solves the general relativistic hydrodynamics equations on a 3D numerical grid with Cartesian coordinates. The code has been constructed within the framework of the `Cactus Computational Toolkit` (see `www.cactuscode.org` for details), devel-

oped at the Albert Einstein Institute (Golm), which provides high-level facilities such as parallelization, input/output, etc., but also the solution of the Einstein equations with matter terms being provided by the Whisky code.

In this paper we briefly discuss the main features of Whisky and present some tests of its validation. Indeed, validation represents an important aspect of the development of any modern 3D finite-difference code. The reasons for this are rather simple and are related to: *(i)* the lack of precise knowledge of the space of solutions of the coupled system of the Einstein and general relativistic hydrodynamics equations; *(ii)* the likely chance that coding errors are made in the implementation of the thousands of terms involved in the solution of such a complicated set of coupled partial differential equations; *(iii)* the complexity of the computational infrastructure needed for the use of the code in a massively parallel environment which increases the risk of computational errors.

The tests presented here will show both the accuracy and the convergence of our formulation for the general relativistic hydrodynamics equations, which are coupled to a conformal transverse-traceless formulation of the Einstein equations (Nakamura et al. 1987). They will also show the ability of the code to follow stably the linear and nonlinear dynamics of isolated relativistic stars. More specifically, we will first present results of the linear pulsations of spherical and rapidly rotating stars. The computed frequencies of radial and quasi-radial oscillations will be compared with the corresponding frequencies obtained with lower-dimensional numerical codes, or with alternative techniques such as the Cowling approximation (in which the spacetime is held fixed and only the general relativistic hydrodynamics equations are evolved), or with relativistic perturbative methods. The comparison shows an excellent agreement confirming the ability of the code to extract physically relevant information even from tiny perturbations. The successful determination of the eigenfrequencies for rapidly rotating stars computed with our code is particularly noteworthy since the equivalent problem has not yet been tackled with perturbative techniques.

We will also investigate the nonlinear dynamics of stellar models that are unstable to the fundamental radial mode of pulsation. We show that upon perturbation, the unstable models will either collapse to a black hole, or migrate to a configuration in the stable branch of equilibrium configurations. In the case of a gravitational collapse, we will follow the evolution all the way down to the formation of a black hole, tracking the generation of its apparent horizon. In the case of migration to the stable branch, on the other hand, we will be able to accurately follow the nonlinear oscillations that accompany this process and that can give rise to strong shocks. The ability to simulate large amplitude oscillations is important as we expect a neutron star formed in a supernova core-collapse (Zwerger & Müller 1997; Dimmelmeier et al. 2001) or in the accretion-induced collapse of a white dwarf to oscillate violently in its early stages of life.

We use the signature $(-,+,+,+)$ and units in which $c = G = M_\odot = 1$. Greek indices are taken to run from 0 to 3 and Latin indices from 1 to 3.

2. Basic Equations

The Whisky code has been constructed exploiting the expertise developed in the building of a similar but distinct code which has been described extensively in (Font et al. 2000b, 2002). The development of the Whisky code has benefited from the release of a public version of the general relativistic hydrodynamics code described in Font et al. (2000b), (2002), and developed mostly by the group at the Washington University as part of the NASA Neutron Star Grand Challenge Project (see wugrav.wustl.edu/Codes/GR3D for details).

The Whisky code, however, also incorporates important recent developments regarding, in particular, new numerical methods for the solution of the hydrodynamics equations. These include: *(i)* the Piecewise Parabolic Method (PPM) (Colella & Woodward 1984) and the Essentially Non-Oscillatory (ENO) methods (Harten et al. 1987) for the cell reconstruction procedure; *(ii)* the Harten-Lax-van Leer-Einfeldt (HLLE) (Harten et al. 1983) approximate Riemann solver, the Marquina flux formula (Aloy et al. 1999b); *(iii)* the analytic expression for the left eigenvectors (Ibáñez et al. 2000) and compact flux formulae (Aloy et al. 1999a) for the Roe Riemann solver and the one using the Marquina flux formula; *(iv)* the possibility to couple the general relativistic hydrodynamics equations with a conformally decomposed 3-metric. The incorporation of these new numerical techniques in the code has lead to a much improved ability to simulate relativistic stars, as will be shown in the section devoted to the tests. The interested reader may also refer to Font et al. (2000b, 2002) for more details about the general formulation and the results obtained with the similar, distinct code.

While the Cactus code provides at each time step a solution of the Einstein equations (see Alcubierre et al. (2000) for the validation of the Cactus code for the spacetime evolution)

$$G_{\mu\nu} = 8\pi T_{\mu\nu} \ , \tag{1}$$

where $G_{\mu\nu}$ is the Einstein tensor and $T_{\mu\nu}$ is the stress-energy tensor, the Whisky code provides the time evolution of the hydrodynamics equations, expressed through the conservation equations for the stress-energy tensor $T^{\mu\nu}$ and for the matter current density J^{μ}

$$\nabla_\mu T^{\mu\nu} = 0 \ , \qquad \nabla_\mu J^{\mu} = 0. \tag{2}$$

An important feature of the Whisky code is the implementation of the so called *Valencia formulation* of the hydrodynamics equations (Martí et al. 1991; Banyuls et al. 1997; Ibáñez et al. 2000), in which the set of equations (2) is written in hyperbolic, flux-conservative form

$$\partial_t \mathbf{q} + \partial_i \mathbf{f}^{(i)}(\mathbf{q}) = \mathbf{s}(\mathbf{q}), \tag{3}$$

where the right hand side (the source terms) depends only on the metric and on the stress-energy tensor, vanishing in a flat spacetime, where the strict hyperbolicity is recovered. In order to write system (2) in the form of system (3), the *primitive* hydrodynamical variables (i.e. the rest mass-density ρ, the pressure p, the fluid 3-velocities v^i, the internal energy density ϵ and the Lorentz factor W) are mapped to the so called *conserved* variables $\mathbf{q} \equiv (D, S^i, \tau)$ via the relations

$$\begin{aligned} D &\equiv \sqrt{\gamma} W \rho \ , \\ S^i &\equiv \sqrt{\gamma} \rho h W^2 v^i \ , \\ \tau &\equiv \sqrt{\gamma}\left(\rho h W^2 - p\right) - D \ , \end{aligned} \tag{4}$$

where γ is the determinant of the spatial 3-metric γ_{ij} and $h \equiv 1+\epsilon+p/\rho$ is the specific enthalpy. The Lorentz factor is defined in terms of the velocities and of the 3-metric as $W = (1 - \gamma_{ij} v^i v^j)^{-1/2}$. Note that only five of the primitive variables are independent.

Finally, an equation of state is used to relate the pressure to the rest mass density and to the energy density. The code can use any equation of state, but presently only a polytropic equation of state of the type

$$p = K \rho^{\Gamma} \ , \tag{5}$$

an "ideal fluid" equation of state

$$p = (\Gamma - 1) \rho \, \epsilon \tag{6}$$

and a hybrid equation of state as described in Zwerger (1995) have been implemented. For more details on this formulation, see also the review by Font (2000).

An important feature of the Valencia formulation is that it is possible to extend to relativistic hydrodynamics the powerful numerical methods developed in classical hydrodynamics; in particular, our code

takes advantage of the High Resolution Shock Capturing (HRSC) properties of Godunov type methods (Godunov 1959). For a full introduction to HRSC methods see Laney (1998), Toro (1999) and LeVeque (1998).

3. Numerical Techniques

The time update of all the equations, general relativistic hydrodynamics and Einstein, are performed with the *Method of Lines* (MoL) (Laney 1998; Toro 1999). The method of lines is a procedure to transform a set of partial differential equations such as (3) into a set of ordinary differential equations. This is done by integrating equations (3) over space in every computational cell defined by its position (x_i, y_j, z_k)

$$\begin{aligned}\frac{\mathrm{d}}{\mathrm{d}t}(\widetilde{\mathbf{q}}) = \mathbf{L}(\widetilde{\mathbf{q}}) = \iiint \mathbf{s}\,\mathrm{d}^3x + \\ + \int_{y_{j-1/2}}^{y_{j+1/2}}\int_{z_{k-1/2}}^{z_{k+1/2}} \mathbf{f}^{(1)}(\mathbf{q}(x_{i-1/2}, y, z))\mathrm{d}y\,\mathrm{d}z \\ - \int_{y_{j-1/2}}^{y_{j+1/2}}\int_{z_{k-1/2}}^{z_{k+1/2}} \mathbf{f}^{(1)}(\mathbf{q}(x_{i+1/2}, y, z))\mathrm{d}y\,\mathrm{d}z \\ + \ \dots\ ,\end{aligned} \tag{7}$$

where $\widetilde{\mathbf{q}}$ is the spatially integrated vector of conserved variables, i.e.

$$\widetilde{\mathbf{q}} \equiv \int \mathbf{q}\ \ \mathrm{d}x\,\mathrm{d}y\,\mathrm{d}z \tag{8}$$

and $\mathbf{f}^{(i)}$ is the i-th component of the flux five-vector $\mathbf{f}$.

Several time-integrators are available in our implementation of MoL and the order of accuracy of the solution of the ordinary differential equation (7) is the same as the truncation order of the integrator employed, provided that the discrete operator $\mathbf{L}$ is of the same order in space and at least first-order accurate in time.

In our implementation of MoL, the right hand side operator $\mathbf{L}(\widetilde{\mathbf{q}})$ is simplified by approximating the integrals with the midpoint rule to get

$$\mathbf{L}(\widetilde{\mathbf{q}}) = \mathbf{s}_{i,j,k} + \mathbf{f}^{(1)}_{i-1/2,j,k} - \mathbf{f}^{(1)}_{i+1/2,j,k} + \cdots\ . \tag{9}$$

Given this simplification, the calculation of the right hand side of (7) splits into the following parts:

1. Calculation of the *source terms* $\mathbf{s}(\mathbf{q}(x_i, y_j, z_k))$ at all the grid points.
2. *Reconstruction* of the data $\mathbf{q}$ to both sides of a cell boundary. In this way, two values $\mathbf{q}_{_L}$ and $\mathbf{q}_{_R}$ of $\mathbf{q}_{i+1/2,j,k}$ are determined at cell boundary; $\mathbf{q}_{_L}$ is obtained from cell i (left cell) and $\mathbf{q}_{_R}$ from cell $i+1$ (right cell). The code implements several reconstruction methods. In particular, as Total Variation Diminishing (TVD) methods we have implemented "minmod", van Leer monotonized centered (van Leer 1979) and Superbee (Toro 1999). Additional reconstruction methods are: arbitrary order ENO methods (Harten et al. 1987) and the Piecewise Parabolic Method (Colella & Woodward 1984), which is a third order accurate in space. As mentioned below, PPM has emerged as our actual best choice for all the test evolutions we present here.
3. Solution at cell boundary of the *Riemann problem* (LeVeque 1998; Toro 1999; Laney 1998) having the values $\mathbf{q}_{_{L,R}}$ as initial data.
4. Calculation in each coordinate direction (x, y, z) of the *inter-cell flux* $\mathbf{f}^{(x)}(\mathbf{q}_{i+1/2,j,k})$, $\mathbf{f}^{(y)}(\mathbf{q}_{i,j+1/2,k})$, $\mathbf{f}^{(z)}(\mathbf{q}_{i,j,k+1/2})$, that is the flux across the boundary between a cell (e.g. the i-th) and its closest neighbour (e.g. the $(i+1)$-th).
5. *Recovery* of the primitive variables and computation of the stress-energy tensor for use in the Einstein equations.

As a result of steps 1. – 4., the core of the Whisky code is effectively represented by two routines. One that reconstructs the function $\mathbf{q}$ at the boundaries of a computa-

tional cell and another one that calculates the inter-cell flux $\mathbf{f}$ at this cell boundary.

As for the reconstruction methods, a similar variety is present for the approximate Riemann solvers implemented in the Whisky code. More specifically, are available the fast HLLE (Harten et al. 1983) and the widespread Roe (Roe 1981) solvers as well as the accurate Marquina flux formula (Aloy et al. 1999b), which is used to solve the Riemann problem in a way that differs from the Roe solver only at sonic points, where the Roe solver has problems. The Roe-based approximate Riemann solvers need the computation of the eigenvalues and eigenvectors (from both the right and left cell) of the linearized Jacobian matrices $\mathbf{A}_{_L}$ and $\mathbf{A}_{_R}$ given by $\mathbf{f}_{_L} = \mathbf{A}_{_L}\mathbf{q}_{_L}$ and $\mathbf{f}_{_R} = \mathbf{A}_{_R}\mathbf{q}_{_R}$. We have implemented the analytic expression for the left eigenvectors (Ibáñez et al. 2000), thus avoiding the computationally expensive inversion of the three 5×5 matrices of the right eigenvectors, associated to each spatial direction. This implementation brings a 40% reduction of the computational time spent in the solution of the hydrodynamics equations. However, in evolutions involving also the time integration of the Einstein equations, this is reduced to a 5% decrease in computational cost. This is due to the fact that the largest part of the time is spent in the update of the spacetime field variables.

4. Numerical Tests

As mentioned above several tests have been performed to assess the stability and accuracy of our code. The results obtained so far are very encouraging and already during these preliminary steps some new physical results have been achieved.

First of all, we consider a standard shock tube test, setting as initial data a global Riemann problem, i.e. one in which the initial discontinuity is orthogonal to the main diagonal of the cubic grid. More precisely the initial data consist of a left and

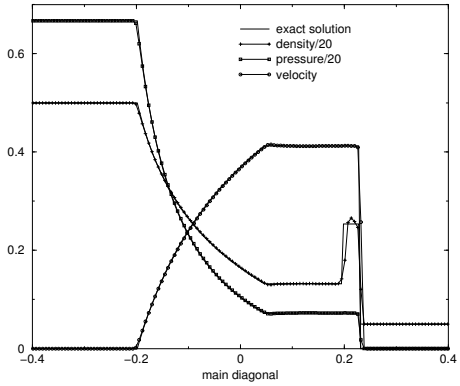

Fig. 1. Solution of a Riemann problem set on the main diagonal of the cubic grid. The figure shows the comparison of the hydrodynamical variables evolved by Whisky, indicated with symbols, with the exact solution. The numerical simulation was obtained with the van Leer reconstruction method and the Roe solver, on a 140^3 grid.

right state with values

$$\begin{aligned} \rho_R &= 1; \;\; p_R = 1.666 \times 10^{-6}; \;\; v_R = 0 \\ \rho_L &= 10; \;\; p_L = 1.333; \qquad\quad v_L = 0 \end{aligned}$$

In Fig. 1 we show the solution at a given time together with the exact solution. The excellent agreement of the two sets of curves is particularly remarkable if one bears in mind that the initial shock is placed on the main diagonal of the cubic grid, so that the evolution is fully 3-dimensional.

Next, we consider the evolution of stable relativistic polytropic spherical (TOV) stars. As this is a static solution, no evolution is expected. Yet as shown in Fig. 2, both a small periodic oscillation and a small secular increase of the central density of the star are detected during the numerical evolution of the equations. Both effects have, however, a single explanation. Since the initial data contains also a small truncation error, this is responsible for triggering radial oscillations which appear as periodic variations in the central density. As the resolution is increased, the truncation

error is reduced and so is the amplitude of the oscillation. The secular growth, on the other hand, is a purely numerical problem, probably related to the violation of the constraint equations. As for the oscillations, also the secular growth converges to zero with increasing resolution. The convergence properties of the code are also clearly shown in the growth of the Hamiltonian constraint violation (Fig. 3), where we can see that almost second-order convergence is achieved. Note that the convergence rate is not exactly second-order, because the reconstruction schemes are only first-order accurate (Alcubierre et al. 2000) at local extrema (i.e. the center and the surface of the star) thus increasing the overall truncation error.

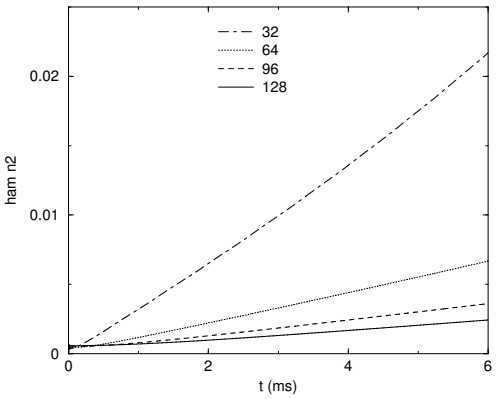

Fig. 3. The L2-norm of the Hamiltonian constraint for the same evolutions as in Fig. 2.

As anticipated, the PPM reconstruction scheme has shown to be more accurate than the TVD ones. This is clear in Fig. 4, in which the results obtained with the PPM method are compared to the best of the TVD methods (i.e. the van Leer one) for a stable TOV run, similar to the previous ones, using 64^3 grid points. Note that the PPM reconstruction is more effective in reducing both the initial truncation error (as shown by the smaller amplitudes in the oscillations) and the secular error (as shown by the small growth rate).

In order to further investigate the accuracy of our implementation of the hydrodynamics equations, we have suppressed the spacetime evolution and solved just the hydrodynamics equations in the fixed spacetime of the initial TOV solution. This approximation is referred to as the "Cowling approximation" and is widely used in perturbative studies of oscillating stars. In this case, in addition to the confirmation of the convergence rate already checked in fully evolved runs, we have also compared the frequency spectrum of the numerically induced oscillation with the results obtained by an independent 2D code (Font et al. 2000a) and with perturbative analyses. In Fig. 5 we show a comparison between the two codes reporting the power spectrum of the central density oscillations computed with the Whisky code and the corresponding frequencies as obtained with perturbative techniques and with the 2D code. Clearly the agreement is very good with an error below 1% in the fundamental frequency. The fact that the frequencies computed with the code coincide with the physical eigenfrequencies calculated through perturbative analysis allows us to study with our code the physical properties of linear normal-modes of oscillation even if such oscillations are generated numerically.

The last test performed in the linear regime consisted of the evolution of rapidly rotating stars, with angular velocity up to 95% of the allowed mass-shedding limit for uniformly rotating stars. The initial data routines have been adapted from the RNS code (Stergioulas & Friedman 1995). As in the previous tests the Hamiltonian constraint shows a convergence rate of nearly second-order everywhere, except at the surface and the center of the star. In analogy with the nonrotating case, the truncation error triggers quasi-radial oscillations in the star. Such pulsations converge to zero with increasing resolution. Determining the frequency spectrum of fully relativistic and rapidly rotating stars is an important scientific achievement, allowing the investiga-

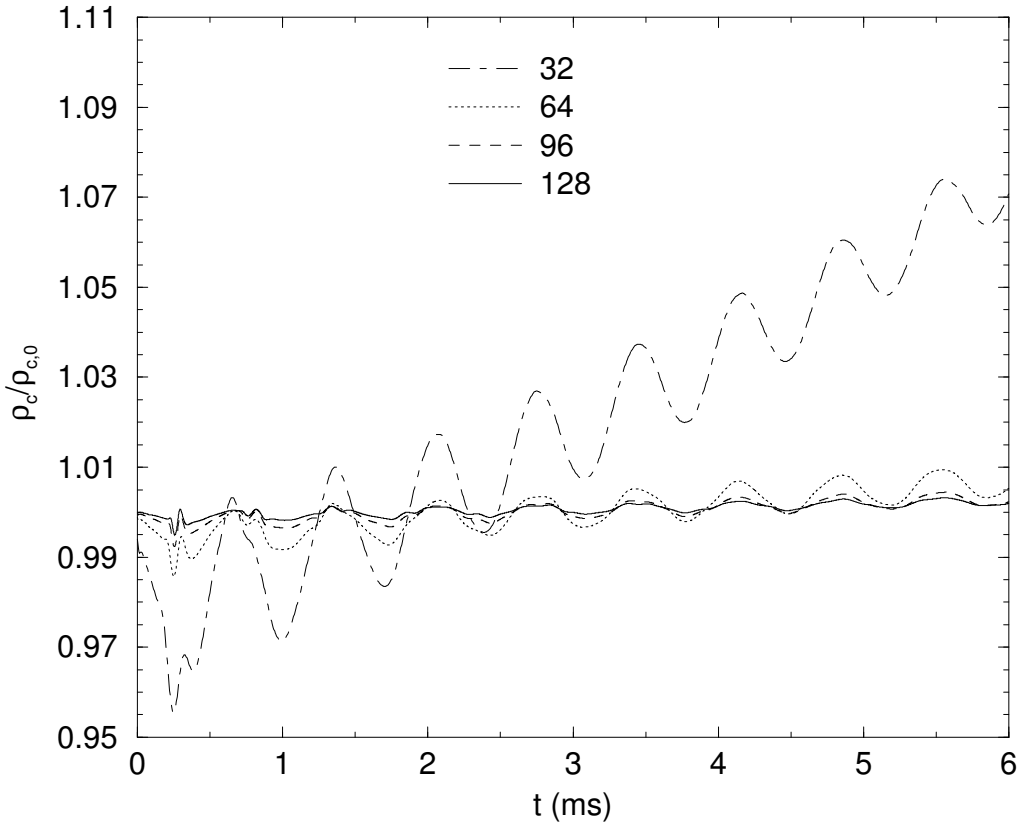

Fig. 2. Central mass-density, normalized to the initial value, in a stable TOV star ($M = 1.4\,M_\odot$ and polytropic index $\Gamma = 2$) evolution at different resolutions. PPM and Marquina were used for all runs.

tion of a parameter space which is astrophysically relevant but too difficult to treat with current perturbative techniques.

Note that a number of small improvements on the boundary and gauge conditions have allowed us to extend considerably the timescale of our evolutions of stable rapidly rotating stars, which can now be evolved for about 10 ms, that is for several rotational periods (Stergioulas 2002).

We now consider tests of the nonlinear dynamics of isolated spherical relativistic stars. To this purpose we have constructed TOV solutions that are placed on the unstable branch of the equilibrium configurations (see inset of Fig. 6). The truncation error in the initial data for a TOV is sufficient to move the model to a different configuration and in `Whisky` this leads to a rapid migration toward a stable configuration of equal rest-mass but smaller central density. Such a violent expansion produces large amplitude radial oscillations in the star that are either at constant amplitude if the polytropic equation of state (5) is used, or are damped through shock heating if the ideal fluid equation of state (6) is used. This is summarized in Fig. 6, which shows the time series of the normalized central density for a TOV. We also show that the asymptotic central density tends to a

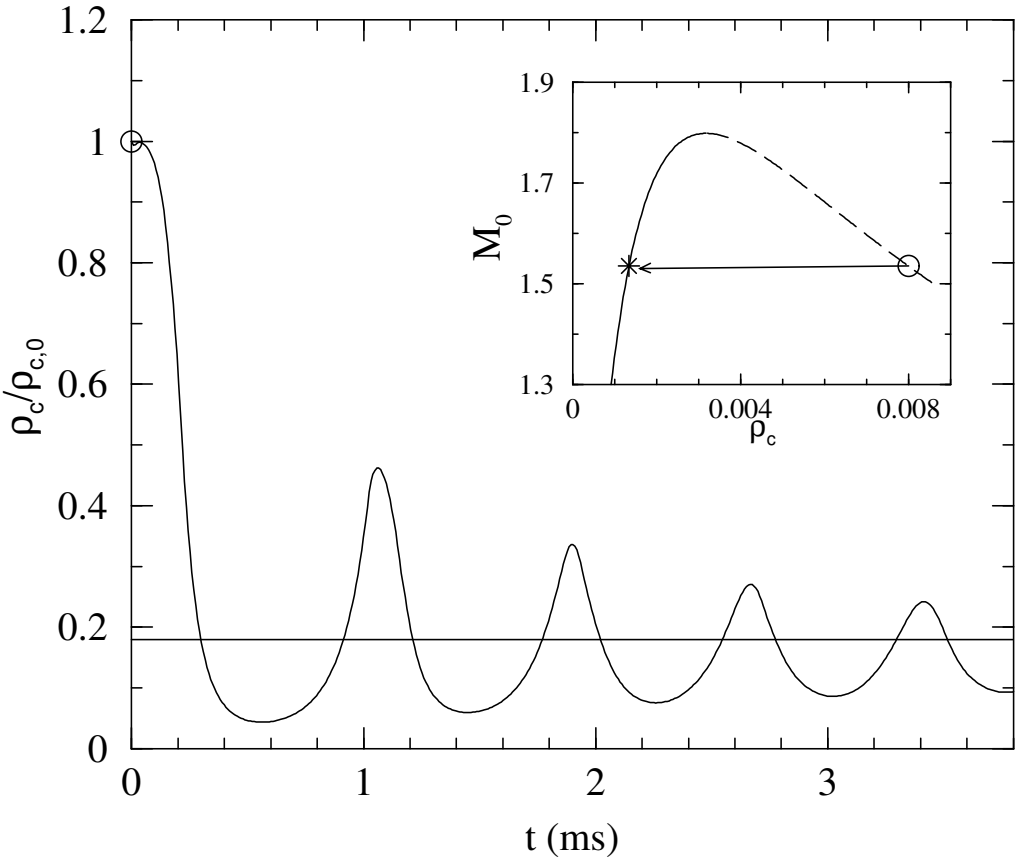

Fig. 6. Normalized central mass-density evolution of an $M = 1.4\,M_{\odot}$, $\Gamma = 2$ unstable TOV star performed with 96^3 grid points.

value corresponding to a rest-mass slightly smaller than the initial one (straight line). This is the energy loss due to the internal dissipation.

An alternative solution for the unstable model is that of a gravitational collapse. In this case, in fact, the initial star does not expand but rather moves to increasingly larger density configurations, finally forming a black hole. In order to study the gravitational collapse of the unstable configuration, the introduction of a density perturbation in the initial model is necessary. A very small one of the order of 1% with dependence $\cos(\pi r/2r_s)$, where r is the coordinate distance from the center and r_s its value on the surface, is sufficient to overcome the effects of the truncation error and induce the star to collapse. Note that after adding the perturbation to the initial configuration, the constraint equations are solved to provide initial data which are a solution to the Einstein equations. As a summary of the results obtained, we show in Fig. 7 the growth of the horizon mass, tracked with an apparent horizon finder based on the fast-flow algorithm (Gundlach 1998). At $t = 0.246$ ms a black hole forms and an apparent horizon appears. As the remaining stellar material continues to accrete onto the newly formed black hole, its horizon mass increases, finally leveling off

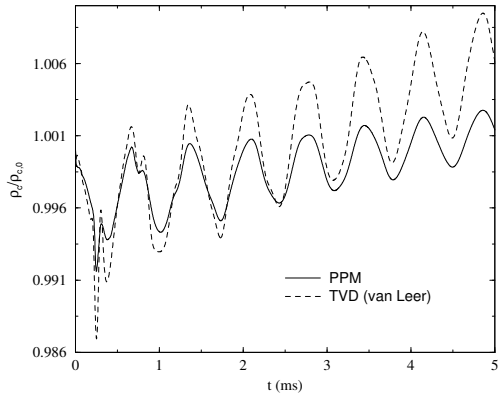

Fig. 4. Central mass-density, normalized to the initial value, in a stable TOV star ($M = 1.4\,M_\odot$ and polytropic index $\Gamma = 2$) evolution with 64^3 grid points. Comparison between PPM and van Leer reconstruction methods.

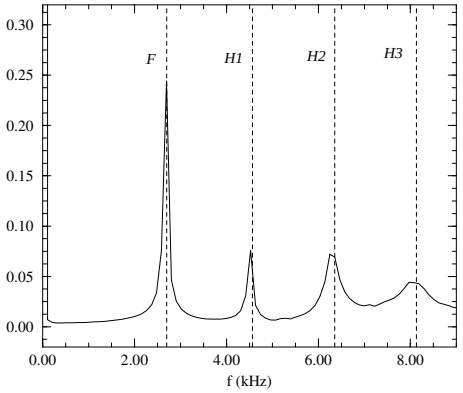

Fig. 5. Fourier transform of the central mass-density evolution of an $M = 1.4\,M_\odot$, $\Gamma = 2$ stable TOV star performed with 128^3 grid points. The units of the vertical axis are arbitrary.

until $t = 0.306$ ms. The subsequent growth of the horizon mass is then only the result of the increasing error due to grid stretching (the radial metric function develops a sharp peak which cannot be resolved accurately enough).

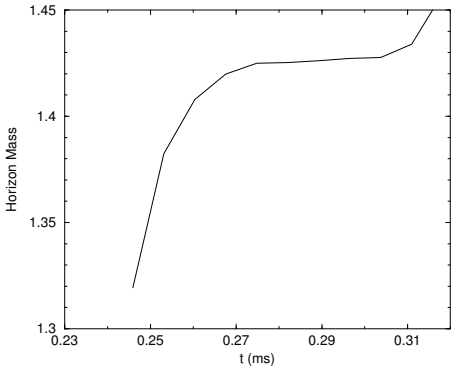

Fig. 7. Horizon mass evolution. The initial rest mass of the TOV star is $M = 1.44\,M_\odot$ and again $\Gamma = 2$.

5. Conclusions

We have illustrated the main features and the present status of our new 3D general relativistic hydrodynamics code. Through a wide set of numerical tests, we have shown both the accuracy and the convergence of our implementation of the formulation of the general relativistic hydrodynamics equations, coupled to a conformal transverse-traceless formulation of the Einstein equations. We have also shown that our code can accurately and stably evolve the linear and nonlinear dynamics of isolated relativistic stars, both for pulsations of spherical and rapidly rotating stars. The computed frequencies of radial oscillations are compared with the corresponding frequencies obtained with other numerical and perturbative techniques and the good agreement among these values is one of the greatest present achievements of our code.

We have also investigated the nonlinear dynamics of stellar models that are unstable to the fundamental radial mode of pulsation, decaying either to a black hole (a collapse which we can follow up to and past the formation of the event horizon) or in a migration to a configuration on the stable branch of equilibrium configurations.

These encouraging results are important premises for the application of the Whisky code to more physical scenarios. Furthermore we are presently working on incorporating in Whisky the use of a fixed mesh refinement. This is an important improvement that will increase the numerical resolution where needed and move the position of the outer boundaries further out in the wave zone, where information on the gravitational wave content of the spacetime can be reliably extracted.

Acknowledgements. It is a pleasure to thank J. Frieben, J. A. Font, José M$^{\underline{a}}$. Ibáñez, F. Löffler, E. Seidel and N. Stergioulas, who have participated to the development and testing of the code. Special thanks also go to Roberto Capuzzo Dolcetta for promoting the first of this series of conferences. Financial support for this work has been provided by the MIUR and EU Network Programme (Research Training Network contract HPRN-CT-2001-01172). The computations were performed on the Beowulf Cluster for numerical relativity *"Albert100"*, at the University of Parma.

References

Alcubierre, M., et al. Phys. Rev. D **62**, 044034 (2000)

Aloy, M. A., Pons, J. A., Ibáñez, J. M., Comput. Phys. Commun., **120**, 115 (1999)

Aloy, M. A., Ibáñez, J. M., Martí, J. M., Müller, E., Astroph. J. Supp., **122**, 151 (1999)

Banyuls, F. Font, J.A. Ibáñez, J.M, Martí, J.M. and Miralles, J.A. Astrophys. J, **476**, 221 (1997)

Colella, P., Woodward, P. R., J. Comput. Phys., **54**, 174 (1984)

Dimmelmeier, H., Font, J. A., Müller, E., Astroph. J. Lett., **560**, L163-L166 (2001)

Duez, M.D., Marronetti, P., Shapiro, S.L., Baumgarte, T.W., Physical Review D, submitted (2002), gr-qc/0209102

Font, J. A., Living Rev. Relativity, **3** (2000)

Font, J. A., Stergioulas, N., Kokkotas, K. D., Mon. Not. R. Astron. Soc., **313**, 678 (2000a)

Font, J. A., Miller, M., Suen, W.-M., Tobias, M., Phys. Rev. D, **61**, 044011 (2000b)

Font, J. A., Goodale, T., Sai, I., Miller, M., Rezzolla, L., Seidel, E., Stergioulas, N., Suen, W.-M., Tobias, M., Phys. Rev. D, **65**, 08024 (2002)

Godunov, S. K., Mat. Sb., **47**, 271 (1959)

Gundlach, C., Phys. Rev. D, **57**, 863 (1998)

Harten, A., Engquist, B., Osher, S., Chakrabarty, S. R., J. Comput. Phys., **71**, 231 (1987)

Harten, A., Lax, P. D., van Leer, B., SIAM Rev., **25**, 35 (1983)

Ibáñez, J. M. et al., in "*Godunov Methods: Theory and Applications*", p. 485-503, Toro E. F., Ed., Kluwer Academic/Plenum Publishers, New York (2001)

Laney, C. B., *Computational Gasdynamics*, Cambridge University Press (1998)

LeVeque, R. L., in *Computational Methods for Astrophysical Fluid Flow*, Steiner O. & Gautschy A., Ed., Springer-Verlag (1998)

Martí, J. M., Ibáñez, J. M., Miralles, J. A., Phys. Rev. D, **43**, 3794 (1991)

Nakamura, T., Oohara, K., Kojima, Y., Prog. Theor. Phys. Supp. **90** (1987)

Roe, P. L., J. Comput. Phys., **43**, 357 (1981)

Shibata, M., Uryu, K., Phys.Rev. D **61** 06400 (2000)

Shibata, M., Uryu, K., Prog. Theor. Phys., **107**, 265 (2002)

Stergioulas, N., private communication (2002)

Stergioulas, N., Friedman, J. L., Astroph. J., **444**, 306 (1995)

Toro, E. F., *Riemann Solvers and Numerical Methods for Fluid Dynamics*, Springer-Verlag, 2$^{\text{nd}}$ edition (1999)

van Leer, B. J., J. Comput. Phys., **32**, 101 (1979)

Zwerger, T., PhD thesis, Technishce Universität München, München, Germany (1995)

Zwerger, T., Müller, E., A&A **320**, 209 (1997)